

## Disorder-induced changes of superconducting $T_c$ obtained by low-temperature ion irradiation of simple metals and alloys

W. Miehle, R. Gerber, and P. Ziemann

*Fakultät für Physik, Universität Konstanz, W-7750 Konstanz, Federal Republic of Germany*

(Received 5 June 1991)

By applying low-temperature ( $T < 10$  K) ion irradiation to continuously increase the disorder of Zn, Al,  $\alpha$ -Ga,  $\beta$ -Ga, In, Pb, AuIn<sub>2</sub>, and Al<sub>2</sub>Au films, the corresponding relative changes of the superconducting transition temperature  $\delta t = \Delta T_c / T_{c0}$  was studied as a function of the electrical resistivity  $\rho$ . In all cases, a linear  $\delta t$ -vs- $\rho$  relation is observed over a wide range of resistivities. The corresponding slopes ( $\delta t / \rho$ ) are compared to existing theories and good agreement is found, provided that experimental input parameters are used for the calculations. For Al, by ion-bombarding oxygen-containing films, the influence of these impurities on the value of ( $\delta t / \rho$ ) could be demonstrated. In addition, by repeating vapor-quenching experiments onto liquid-helium-cooled substrates for Zn,  $\alpha$ -Ga, and Al, earlier discrepancies concerning the value of ( $\delta t / \rho$ ) are resolved. Even in cases in which an amorphous phase results by ion irradiation ( $\alpha$ -Ga, AuIn<sub>2</sub>, Al<sub>2</sub>Au), a continuous  $\delta t$ -vs- $\rho$  curve is obtained, emphasizing a universal behavior of  $T_c$  on disorder. But a detailed comparison of disorder produced by different preparation techniques clearly reveals deviations from such universality. This indicates that different types of defects act differently on  $T_c$ .

### I. INTRODUCTION

Experimentally it has long been known that the superconductive transition temperature ( $T_c$ ) can be influenced by introducing disorder into a superconductor. In a large number of metallic alloys, and in some rare cases like Ga even in elemental superconductors, an increasing degree of disorder eventually leads to an amorphous system accompanied by corresponding  $T_c$  changes. Qualitatively one finds that low- $T_c$  materials show a  $T_c$  enhancement while high- $T_c$  materials exhibit a  $T_c$  degradation due to disorder.

Theoretically, as a consequence of Anderson's theorem,<sup>1</sup> a BCS superconductor should not be affected by disorder at all as long as time-reversal invariance holds and neither the density of states (DOS) nor the effective phonon-mediated electron-electron interaction is changed. Consequently, within this framework the observed  $T_c$  changes have to be attributed either to disorder-induced changes of the DOS or of the effective electron-phonon coupling. In simple metals without sharp structures of the DOS near the Fermi energy, changes of the electron-phonon coupling are expected to play the dominant role. Based on this idea, Keck and Schmid<sup>2</sup> calculated the influence of disorder on the electron-phonon coupling constant  $\lambda$  within Eliashberg theory. Neglecting effects of DOS and Coulomb interaction, these authors found an enhancement of  $T_c$  for disordered low- $T_c$  superconductors. More specifically, if the disorder is characterized by the corresponding electrical resistivity  $\rho$ , a linear increase  $\Delta T_c / T_{c0} \sim \rho$  is obtained at small  $\lambda$  values with slopes  $(\Delta T_c / T_{c0}) / \rho$  of the order of the experimentally observed values. But clearly, this theory has not been able to describe the experimentally observed  $T_c$  degradation for strong-coupling supercon-

ductors. Here, in the case of transition metals and  $A15$  compounds, the disorder-induced  $T_c$  decrease has been attributed to DOS (Ref. 3) or to Coulomb effects.<sup>4</sup> In addition, the importance of the normal self-energy has been realized.<sup>5,6</sup> Taking the effects of the normal self-energy into account and including Coulomb interaction, Belitz was able to extend the theory of disorder-induced  $T_c$  changes into the strong-coupling regime.<sup>7</sup> The main result of this extension is that it reproduces the experimentally observed trend, i.e., for small  $\lambda$  values, a  $T_c$  enhancement is obtained while large  $\lambda$  values result in a  $T_c$  decrease. To arrive at this result, the disorder renormalizations were calculated to first order within a jellium model. As a consequence, DOS effects are not included in this theory and, for weak disorder, a universal linear behavior of the relative  $T_c$  changes  $\Delta T_c / T_{c0}$  as a function of the resistivity  $\rho$  is found. Quantitatively, the scale of the resistivity is set by the Mott resistivity  $\rho_M$  of a metal. By using two sets of jellium input data representing simple metals and transition-metal- $A15$ -material compounds, respectively, Belitz obtained reasonable agreement between his theory and experimental data over the full range of  $\lambda$  values  $0 \leq \lambda \leq 2$ . But even within the more restricted range  $\lambda \leq 1$ , for some metals like Al, Ga, and In, strong deviations of the experimental results from the standard Belitz curve occur. These deviations might well be a consequence of experimental difficulties. For instance, a prominent technique to produce disorder is quenching. Here, metals like In, Ga, Al are prepared by evaporation onto liquid-He-cooled substrates<sup>8,9</sup> followed by annealing steps. Especially, if an amorphous phase results by this technique, as for Ga, only the starting and final values of  $\rho$  and  $T_c$  are determined and the data cannot be checked for the linear ( $\Delta T_c / T_{c0}$ )-vs- $\rho$  behavior predicted by theory. The slope deduced from the starting

and final values might thus be of no use for a quantitative comparison to theory. Even if the highly disordered as-quenched state can be stepwise annealed thereby reducing the disorder, by this procedure the various types of defects, of which each may act differently on  $T_c$ , disappear at different temperatures leading to more curved  $T_c$ -vs- $\rho$  curves. As will be shown, such a behavior appears to be present in the case of In. It then indicates that a universal description of disorder in terms of resistivity is only a first approximation. Rather, different types of defects, though producing the same value of  $\rho$ , can result in different  $T_c$  values. In this way, considerable variations of the slopes  $(\Delta T_c/T_{c0})/\rho$  are obtained when the results of different preparation techniques are compared, though the relative differences of the  $T_c$  values usually are small. It is the aim of the present paper to provide experimental data for eight different superconducting systems, into which disorder could be gradually introduced by the same technique in all cases. For this purpose, ion irradiation at low temperatures combined with *in situ* measurements of  $T_c$  and  $\rho$ , has been applied. The corresponding experimental details will be given in Sec. II. To allow a quantitative comparison to theory, systems have to be chosen where DOS effects are expected to be negligible. Furthermore, one should concentrate on the regime of weak disorder, i.e.,  $\rho < 100 \mu\Omega \text{ cm}$ . For these reasons, the following systems were chosen: the elemental superconductors Al, Zn, In,  $\alpha$ -phase Ga,  $\beta$ -phase Ga, Pb, and the intermetallic compounds AuIn<sub>2</sub> and Al<sub>2</sub>Au. For  $\alpha$ -phase Ga, AuIn<sub>2</sub>, and Al<sub>2</sub>Au, by increasing disorder, eventually an amorphous phase is obtained, while in the other cases the polycrystalline state is preserved.

The experimental results are presented in Sec. III for each system separately. Emphasis is put on the question whether a linear  $T_c$ - $\rho$  relation can be used to describe the data. In such cases, the corresponding slopes are compared to the theoretical values calculated using realistic input parameters.

## II. EXPERIMENT

In all cases of this study, the disorder necessary to induce  $T_c$  changes is introduced into the samples by low-temperature ion irradiation. For this purpose, films of a typical thickness  $D = 80 \text{ nm}$  are bombarded with inert ions (mostly Ar<sup>+</sup>). The energy of the projectiles is chosen such that the corresponding projected range of the ions is larger than the film thickness. In this way, any significant implantation of the bombarding species can be avoided (the concentration of implanted atoms was kept below 1.5 at. % in all cases) and quite homogeneous radiation damage profiles are obtained. An example is given in Fig. 1, where the nuclear energy loss  $(dE/dx)_n$  of Ar<sup>+</sup> ions (275 keV) within a Zn film is shown. This damage profile, calculated by the TRIM code,<sup>10</sup> exhibits a variation of less than 17% over the film depth. Such homogeneous profiles are necessary to guarantee a correct calculation of the film resistivity from its measured resistance. Additionally, shown in Fig. 1 is the concentration profile of implanted Ar atoms. Even after irradiation of a high

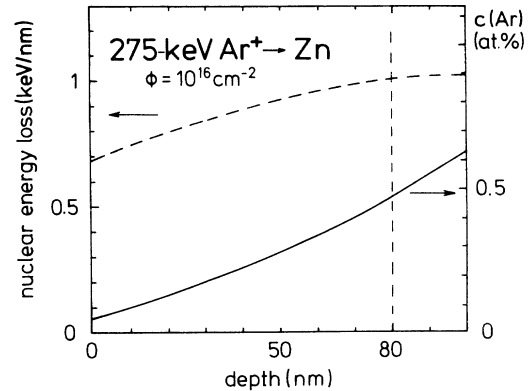


FIG. 1. Typical ion-irradiation conditions exemplified by the 275-keV Ar<sup>+</sup> bombardment of Zn films (thickness 80 nm). The damage profile is given by the dashed curve (left scale). The profile of the implanted Ar atoms corresponding to a total fluence of  $10^{16} \text{ cm}^{-2}$  is represented by the solid line (right scale). Both curves are calculated using the TRIM code (Ref. 10).

fluence ( $10^{16} \text{ Ar/cm}^2$ ), the implanted Ar concentration is well below 1 at. %. To further exclude any additional influence of the implanted species, Zn and In films were also implanted with Ar<sup>+</sup> (150 keV). In both cases no specific implantation effect on the  $T_c$  changes could be detected.

In order to achieve a high degree of disorder by the irradiation technique, the samples must be kept at low temperatures during bombardment to avoid annealing. In the following, all irradiations were performed at 4.2 K (nominal temperature of the sample holder) and the beam current was reduced appropriately to guarantee a film temperature of less than 10 K during bombardment. Temperatures were determined by a commercial Ge-resistance thermometer and for the *in situ* measurement of the irradiation-induced resistance changes the usual four-point technique was applied. In this way, also, the corresponding  $T_c$  changes were determined resistively. Since some of the systems studied exhibit  $T_{c0}$  values well below 1 K, two sets of experiments have been performed: Al<sub>2</sub>Au and Zn films were ion bombarded within a <sup>3</sup>He-<sup>4</sup>He dilution cryostat with a lowest attainable temperature of 150 mK, while the other systems were irradiated within a <sup>4</sup>He cryostat (lowest attainable temperature 1.2 K). A more detailed description of both types of irradiation cryostats are given in Ref. 11.

Except for Al, all other systems were prepared *in situ* within the irradiation cryostats by evaporation from resistively heated boats. In case of the AuIn<sub>2</sub> and Al<sub>2</sub>Au alloys, bulk samples are produced first and, after grinding, small grains (with diameter  $\leq 0.28 \text{ mm}$ ) are flash evaporated to avoid changes of the stoichiometry due to fractional evaporation. The above compounds were evaporated in this way onto glass substrates held at 77 K resulting in amorphous phases<sup>12,13</sup> with well-defined recrystallization temperatures  $T_K$  ( $T_K = 210 \text{ K}$  for Al<sub>2</sub>Au,  $T_K = 190 \text{ K}$  for AuIn<sub>2</sub>). After recrystallization of the evaporated amorphous phase and annealing up to 300 K, the films are recooled to 4.2 K and ion irradiated. The Al films were prepared *ex situ* within a separate UHV

chamber by electron-gun evaporation. Here, the background pressure during evaporation could be kept below  $10^{-8}$  mbar, while within the cryostates the corresponding pressures were in the  $10^{-6}$ -mbar range. Since the superconducting properties of Zn, and especially of Al, are sensitive to the amount of oxygen present within a film, these metals were also evaporated under controlled pressures of oxygen. The resulting oxygen concentration within the films could be determined by Rutherford backscattering (RBS). Impurities like oxygen also play an important role in the ion-irradiation experiments, since they are able to chemically stabilize defects leading to higher irradiation-induced resistivities as compared to pure samples.<sup>14</sup> This again could result in erroneous  $T_c$ -vs- $\rho$  relations. To get a quantitative estimate of such an effect, Al films with deliberately incorporated amounts of oxygen were ion bombarded in the same way as the pure samples and the corresponding  $T_c$  and  $\rho$  changes were determined. In the following section the results are reported for each system separately.

### III. RESULTS

#### A. Zn

All Zn films (eight samples) were evaporated from a resistively heated Ta boat within the  $^3\text{He}$ - $^4\text{He}$  cryostat onto glass substrates held at 150 K. Typical evaporation rates were 6 nm/s at a background pressure in the  $10^{-6}$ -mbar range. After annealing the films at 300 K (RT), they were recooled to liquid-He temperature for the irradiation experiments. From the temperature dependence of the resistance  $R(T)$  during cooling, the film thickness could be determined. Typical thicknesses ranged between 60 and 80 nm. The resistance ratios  $r=R(\text{RT})/R(4.2\text{ K})$  of the films were found as  $2.7 \leq r \leq 3.6$  and the absolute values of the resistivity  $\rho(4.2\text{ K})$  were in the range  $2.4\ \mu\Omega\text{ cm} \leq \rho(4.2\text{ K}) \leq 3.70\ \mu\Omega\text{ cm}$ . The transition temperature to superconductivity  $T_{c0}$  exhibited only a small variation from film to film resulting in an average value of  $\langle T_{c0} \rangle = 0.81 \pm 0.01\text{ K}$ .

Three types of ion bombardment were performed:  $\text{Ar}^+$  irradiation with 275 keV (projected range  $R_p$  of the ions larger than film thickness  $D$ ),  $\text{Ar}^+$  implantation with 150 keV ( $R_p < D$ ), and  $\text{He}^+$  irradiation with 200 keV ( $R_p \gg D$ ). The results of all ion bombardments are summarized in Fig. 2, where the relative  $T_c$  changes  $\delta t = \Delta T_c / T_{c0}$  are plotted versus the resistivity  $\rho$ . Such a representation allows a direct comparison to the theories of Belitz<sup>7</sup> and Keck and Schmid,<sup>2</sup> who predict a linear relation for these quantities. Indeed, the data in Fig. 2 (different symbols represent different samples) can be satisfactorily described by such a linear relation with a slope  $(\delta t / \rho) = 16.5\ (\text{m}\Omega\text{ cm})^{-1}$ . Within the scatter of the data around the average solid line in Fig. 2, no difference is found between Ar irradiation (open symbols), Ar implantation (solid symbols), and the He irradiation (crosses). On the other hand, the production of different types of defects are expected under these different bombarding

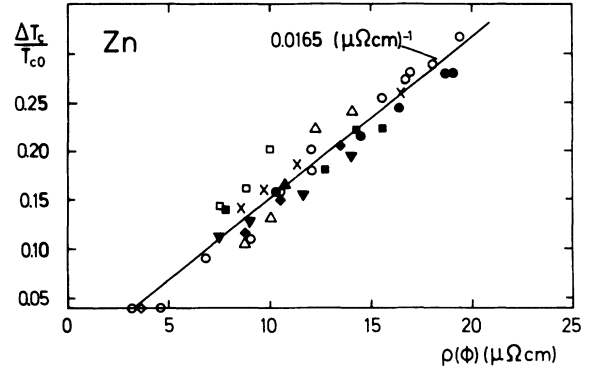


FIG. 2. Relative changes of the superconducting transition temperature  $\Delta T_c / T_{c0}$  induced by low-temperature ( $T < 10\text{ K}$ )  $\text{Ar}^+$  bombardment of Zn films as a function of the electrical resistivity  $\rho$ . Different symbols stand for different samples [open symbols, Ar irradiation (275 keV); solid symbols, Ar implantation (150 keV); crosses, He irradiation (200 keV)].

conditions. Thus, the observed linear behavior can be interpreted as a “universal” dependence of  $T_c$  on disorder.

For a quantitative comparison to theory, a number of input parameters must be provided: the Debye temperature  $\Theta_D$  and the Debye wave vector  $q_D$ , the Fermi energy  $E_F$ , and the Fermi wave vector  $k_F$ , the inverse Coulomb-screening length  $\kappa$ , the ratio of the longitudinal to the transverse velocity of sound  $c_L / c_T$ , and the Mott resistivity  $\rho_M$ , which is given within a free-electron model (FEM) by  $\rho_M^{\text{FEM}} = (3\pi^2 \hbar) / (k_F e^2)$ . When these properties are known, the input parameters for the theory can be calculated. Adapting the notation of Ref. 7, all necessary input data for Zn are collected in Table I. In this context, the following problem should be noted: though Zn is expected to be free-electron-like,<sup>15</sup> the scattering of electrons leading to resistivity may be strongly influenced by the complicated topology of its Fermi surface<sup>16</sup> making the value of  $\rho_M^{\text{FEM}}$  quite uncertain. On the other hand, the actually observed scattering behavior of the electrons can be quantified by the product  $A^{\text{expt}} = \rho \cdot l$  ( $l$  is the elastic mean free path of the electrons). In the FEM, the corresponding value  $A^{\text{FEM}}$  is given by  $A^{\text{FEM}} = (3\pi^2 \hbar) / (k_F^2 e^2) = \rho_M^{\text{FEM}} / k_F$ . In analogy, we define the value  $\rho_M^{\text{expt}}$  by  $\rho_M^{\text{expt}} = A^{\text{expt}} k_F$ , i.e.,  $k_F$  is given by the FEM value, while  $A^{\text{expt}}$  are experimental values taken from the literature. These values are also included in Table I. The columns  $(\delta t / \rho)_B$  and  $(\delta t / \rho)_{\text{KS}}$  give the theoretical results after Belitz<sup>7</sup> and Keck and Schmid,<sup>2</sup> respectively. Excellent agreement between theory and experiment is obtained if the experimental Mott resistivities are used. For the calculation, the coupling constant  $\lambda$  corresponding to  $T_{c0}$  must be known. For this purpose, McMillan’s  $T_c$  formula,<sup>26</sup> which takes into account Coulomb effects by  $\mu^*$ , is inverted to give  $\lambda_M$ . On the other hand, in the theory of Keck and Schmid,  $\mu^*$  effects are neglected. Thus, for a comparison to this theory, the  $\lambda_0$  value calculated from Ref. 26 with  $\mu^* = 0$  appears more appropriate. Both values are included in Table I. With the above modification both theories deliver identical results for Zn. This agreement between theory and experiment should not be overestimated as can be seen

from the following estimates: the partial derivatives  $\partial(\delta t/\hat{\rho})/\partial x_D$ ,  $\partial(\delta t/\hat{\rho})/\partial y$  and  $\partial(\delta t/\hat{\rho})/\partial(c_L/c_T)^2$  were calculated numerically from Belitz's theory at the point  $x_D=0.44$ ,  $y=0.62$ ,  $(c_L/c_T)^2=2.98$  representing Zn (the results are also included in Table I). Here,  $\hat{\rho}$  is defined by  $\rho/\rho_M$ . Assuming a relative error of 10% for  $x_D$  and  $y$  and 5% for  $(c_L/c_T)^2$ , one calculates by standard error analysis a total absolute error  $\Delta(\delta t/\rho)=10.3$  (m $\Omega$  cm) $^{-1}$  for  $\rho_M=2.8$  m $\Omega$  cm. But even with such a large uncertainty, the theoretical value  $(\delta t/\rho)_B=18\pm 10$  (m $\Omega$  cm) $^{-1}$  lies significantly below the FEM value of 67 (m $\Omega$  cm) $^{-1}$ . In this context, it is important to note that an experimental value of  $60\pm 10$  (m $\Omega$  cm) $^{-1}$  for Zn is quoted by Belitz.<sup>7</sup> This value was obtained by vapor quenching onto liquid-He-cooled substrates.<sup>8</sup> In order to check this value, we have repeated the same type of experiment under improved vacuum conditions. Two films (thicknesses 70 and 67 nm as determined optically by the Tolansky technique) were evaporated onto glass substrates held at 4.2 K (pressure during deposition  $10^{-6}$  mbar) and  $\rho$  and  $T_{c0}$  were determined *in situ*. For the transition temperature we obtained  $T_{c0}=1.33$  and 1.28 K, i.e., only slightly smaller values than 1.39 K reported in Ref. 8. But our resistivities were  $\rho(4.2$  K) $=24.3$  and 25.6  $\mu\Omega$  cm, respectively, i.e., larger by a factor of 2.6 as compared to Ref. 7. In our opinion, this discrepancy can be resolved by noting that, in Ref. 8, a value of  $\rho(273$  K) $=4.8$   $\mu\Omega$  cm is given for Zn, which is then used to calculate the resistivity of the quenched film. But 4.8  $\mu\Omega$  cm is clearly a bulk value, not appropriate for films, which still are disordered even after annealing to RT. In our case, the eight films used for the ion-irradiation experiments exhibited an average value  $\rho(\text{RT})=9.8$   $\mu\Omega$  cm, which is larger by a factor of 2.1, thus practically compensating the above factor 2.6. As a consequence, we obtain  $\delta t/\rho=29$  (m $\Omega$  cm) $^{-1}$  rather than 60 (m $\Omega$  cm) $^{-1}$  for quench-condensed Zn films. But even this smaller value is significantly larger than the slope obtained for ion-induced disorder [ $16.5$  (m $\Omega$  cm) $^{-1}$ ]. Thus, one has to conclude that different techniques lead to different types of disorder, each acting differently on  $T_c$ . Consequently, at a given  $\rho$  value, different  $T_c$  values can be observed proving that any universal  $T_c$ -vs- $\rho$  relation must be taken as a more or less satisfying approximation.

### B. Ga

Ga represents one of the few cases where a metallic element can be forced into the amorphous phase by quenching its vapor onto a liquid-He-cooled substrate.<sup>8</sup> The amorphous ( $\alpha$ ) phase exhibits an electrical residual resistivity of  $\rho=33$   $\mu\Omega$  cm and a  $T_{c0}$  value of 8.5 K, but it is stable only up to  $T_K=17$  K, where it transforms into the metastable crystalline  $\beta$ -Ga phase.<sup>17</sup> This  $\beta$ -Ga shows a much lower resistivity of  $\rho=3$   $\mu\Omega$  cm and a  $T_{c0}$  value of 6.3 K. Eventually, at 60 K,  $\beta$ -Ga transforms into the stable  $\alpha$  phase with a residual resistivity of  $\rho=12$   $\mu\Omega$  cm and  $T_{c0}=1.07$  K. From earlier ion-irradiation experiments of Ga films it is well known<sup>17,19</sup> that low-temperature ion bombardment of  $\alpha$ -Ga leads to the amorphous phase, while  $\beta$ -Ga can only be slightly disor-

TABLE I. Input data for Zn.

$\Theta_D$ (K)	$k_F$ ( $10^8$ cm $^{-1}$ )	$q_D$ ( $10^8$ cm $^{-1}$ )	$\kappa$ ( $10^8$ cm $^{-1}$ )	$T_{c0}$ (K)	$\rho_M^{\text{FEM}}$ ( $\mu\Omega$ cm)	$\rho_M^{\text{expt}}$ ( $\mu\Omega$ cm)	$A^{\text{expt}}$ ( $10^{-12}$ $\Omega$ cm $^2$ )	$\rho_M^{\text{expt}}$ ( $\mu\Omega$ cm)	$(\delta t/\rho)_B$ (1/m $\Omega$ cm)	$(\delta t/\rho)_{\text{KS}}$ (1/m $\Omega$ cm)	$(\delta t/\rho)_{\text{expt}}$ (1/m $\Omega$ cm)			
322 <sup>a</sup>	1.58 <sup>b</sup>	1.38 <sup>b</sup>	1.95 <sup>b</sup>	0.81 <sup>c</sup>										
5.83 <sup>b</sup>	0.62	0.44	2.98 <sup>d</sup>	770 <sup>e</sup>					67	$\lambda_M=0.381^h$	$\lambda_0=0.227^i$			
5.83 <sup>b</sup>	0.62	0.44	2.98 <sup>d</sup>		18 <sup>c</sup>	2844		11	18.5	11	16.5 $\pm$ 1			
5.83 <sup>b</sup>	0.62	0.44	2.98 <sup>d</sup>		12 <sup>c</sup>	1896		16.5	27.7	16.5	27.7			
											$\partial(\delta t/\rho)/\partial y^f$	$\partial(\delta t/\rho)/\partial x_D$	$\partial(\delta t/\rho)/\partial(c_L/c_T)^2$	$\partial(\delta t/\rho)/\partial T_{c0}$ (K $^{-1}$ )
											-16.4	-561	+54.5	-39

<sup>a</sup>From Ref. 18.

<sup>b</sup>From Ref. 15.

<sup>c</sup>Experimental average of eight Zn films.

<sup>d</sup>From Ref. 20.

<sup>e</sup>From Ref. 21.

<sup>f</sup> $\hat{\rho}=\rho/\rho_M$ .

<sup>g</sup> $\rho_M^{\text{FEM}}=3\pi^2\hbar/k_F e^2$ .

<sup>h</sup>McMillan value.

<sup>i</sup>McMillan value with  $\mu^*=0$ .

dered by this technique, but remains polycrystalline. In the following, the irradiation-induced  $T_c$  changes will be reported for both cases.

The Ga films (typical thickness 40 nm) were prepared *in situ* by evaporation onto liquid-He-cooled glass substrates resulting in the  $\alpha$ -Ga phase. The crystalline phases were obtained from the amorphous-phase by heating to the corresponding crystallization temperature. After recoiling, the crystalline films were irradiated at  $T < 10$  K with different projectiles ( $\text{Ar}^+$ ,  $\text{Kr}^+$ ) and the resulting  $T_c$  and  $\rho$  changes were determined. The results are shown in Fig. 3(a) for  $\alpha$ -Ga bombarded with 350-keV  $\text{Ar}^+$  ions. A linear relation is found between the relative  $T_c$  changes and the resistivity up to  $\rho = 24 \mu\Omega \text{ cm}$  with an exceptional high value of the slope  $(\delta t/\rho) = 545 (\text{m}\Omega \text{ cm})^{-1}$ . For even higher resistivities approaching the amorphous value, a clear deviation from the straight line is observed: while  $T_c$  has reached its amorphous value of 8.5 K, the resistivity can still be increased by the ion bombardment. But this behavior could well be an experimental artifact caused by an inhomogeneous depth profile of the irradiation-induced damage. In such a case, further irradiation leads to a saturation of the resistivity, while the resistive  $T_c$  measurement indicates the highest

$T_c$  value present within the film, i.e., the amorphous value corresponding to the highest damage level. Thus, only the linear part of the curve in Fig. 3(a) is compared to theory. In Fig. 3(b) the corresponding behavior of the crystalline  $\beta$ -Ga is presented. Since the  $\beta$ -Ga films differed in their residual resistivities  $\rho(7 \text{ K})$ , the irradiation-induced  $T_c$  changes  $\delta t$  are plotted versus  $\Delta\rho = \rho(\Phi) - \rho(\Phi=0)$ . Both,  $\text{Ar}^+$  and  $\text{Kr}^+$  irradiations lead to linear  $\delta t$ -vs- $\Delta\rho$  relations, but with slightly different slopes [ $14.9$  and  $20.7 (\text{m}\Omega \text{ cm})^{-1}$ , respectively]. This observation indicates that different defects as produced by different projectiles act differently on  $T_c$  in contrast to the assumption of a universal  $\delta t$ -vs- $\rho$  curve. To compare the experimentally obtained slopes to theory, the input data given in Table II were used. These data refer to the stable  $\alpha$ -Ga phase or were calculated according to the FEM. The most conspicuous parameter in Table II is the ratio  $(c_L/c_T)^2$  exhibiting an exceptionally large value of 16.3. The calculated slope  $(\delta t/\rho)_B$  based on these parameters [ $519 (\text{m}\Omega \text{ cm})^{-1}$ ] is surprisingly close to the experimental one [ $545 (\text{m}\Omega \text{ cm})^{-1}$ ]. Thus, this high value can be mostly traced back to the anomalous high  $(c_L/c_T)$  ratio. It is noteworthy that the results of quench-condensation experiments also give large  $(\delta t/\rho)$  slopes, if the final amorphous values and the starting  $\alpha$ -Ga values are used. In this way, we obtain  $(\delta t/\rho) = 338 (\text{m}\Omega \text{ cm})^{-1}$  in contrast to the value quoted by Belitz<sup>7</sup> [ $40 (\text{m}\Omega \text{ cm})^{-1}$ ]. The slope  $(\delta t/\rho)_{KS}$  calculated after Keck and Schmid using the same input parameters is also included in Table II for completeness.

The results obtained for the metastable  $\beta$ -Ga clearly follow the general trend that higher  $T_{c0}$  values lead to smaller slopes  $(\delta t/\rho)$ . A more detailed comparison to theory is not possible since the necessary experimental input parameters are not available. But it is noteworthy that, by reducing the anomalous high  $(c_L/c_T)^2$  value from 16.3 to the more typical value of 4.7, one obtains a slope  $(\delta t/\rho) = 15 (\text{m}\Omega \text{ cm})^{-1}$  equal to the experimental value found for Ar irradiation. A more physical, though still speculative, estimate is based on the following consideration. Experimentally, one commonly finds  $(c_L/c_T)^2 = 1.8$ . This value was also applied by Belitz for calculating his standard  $(\delta t/\rho)$ -vs- $T_{c0}$  curves.<sup>7</sup> Adopting this value for  $\beta$ -Ga and assuming that the longitudinal velocity of sound  $c_L$  is the same as for  $\alpha$ -Ga [ $c_L^\beta = c_L^\alpha = 3030 \text{ m/s}$  (Ref. 20)], one calculates an average sound velocity  $\langle c \rangle = 2516 \text{ m/s}$ , which is larger by a factor of 1.7 than the corresponding average for  $\alpha$ -Ga. As a consequence, a smaller  $q_D$  value is obtained for  $\beta$ -Ga leading to a smaller input parameter  $x_D = 0.37$  for fixed  $k_F$ . Leaving all other input parameters as given in Table II, one obtains  $(\delta t/\rho)_B = 8 (\text{m}\Omega \text{ cm})^{-1}$  close to the experimental value. Thus, the experimentally observed slopes  $(\delta t/\rho)$  for  $\alpha$ -Ga and  $\beta$ -Ga can be both described by the theory by Belitz applying reasonable sets of input parameters despite their large numerical difference.

### C. Al

It is well known that the transition temperature of Al reacts sensitively to the presence of oxides within the

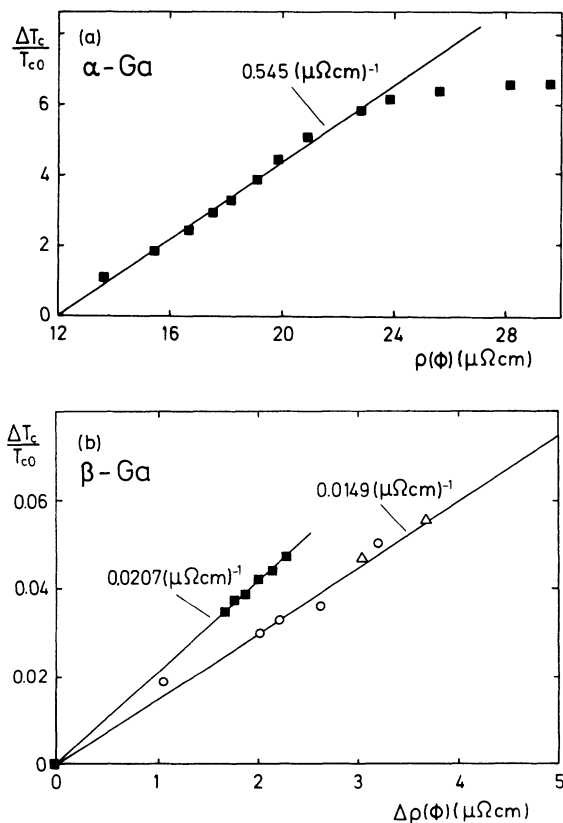


FIG. 3. Relative changes of the superconducting transition temperature  $\Delta T_c/T_{c0}$  induced by low-temperature ( $T < 10$  K) ion bombardment of different modifications of Ga as a function of the electrical resistivity  $\rho$ . (a)  $\text{Ar}^+$  irradiation of an  $\alpha$ -Ga film (350 keV). (b) Irradiation of  $\beta$ -Ga films [open symbols,  $\text{Ar}^+$  irradiation (230 and 275 keV); solid squares,  $\text{Kr}^+$  irradiation (350 keV);  $\Delta\rho = \rho(\Phi) - \rho(0)$ ].

films.<sup>22-24</sup> Furthermore, it has been demonstrated that the irradiation-induced resistivity changes also depend on the oxygen concentration present within the bombarded films.<sup>14,25</sup> To clarify the complex behavior of Al films, previous data<sup>14</sup> are reanalyzed in the form  $\delta t$ -vs- $\rho$  and compared to theories.

The Al films were prepared *ex situ* by evaporation under UHV conditions or under controlled oxygen partial pressures at RT onto glass substrates. The actual concentration of oxygen  $c_O$  present within the films due to this preparation procedure was determined by RBS. Experimental details can be found in Ref. 14. Additionally, Al films were vapor quenched onto liquid-He-cooled substrates and  $c_O$  determined after warming to RT.<sup>25</sup> The average film thickness was 100 nm.

For the low-temperature ion bombardment, Al self-ions ( $Al^{2+}$ , 500 keV) were used ( $R_p > D$ ) and the resulting  $T_c$  and  $\rho$  changes were determined *in situ*. The results of the ion irradiation are shown in Fig. 4. Here  $\delta t$  is plotted versus resistivity  $\rho$  for Al films of different oxygen concentrations  $c_O$  resulting in different residual resistivities prior to the ion bombardment. For all films a linear  $\delta t$ - $\rho$  relation is obtained, but with slopes depending on  $c_O$ . For the purest films ( $c_O < 0.5$  at. %, this limit is given by the resolution of RBS)  $(\delta t/\rho) = 159$  (m $\Omega$  cm)<sup>-1</sup>, for  $c_O = 1.4$  and 3.6 at. % the slope significantly increases up to  $(\delta t/\rho) = 269$  (m $\Omega$  cm)<sup>-1</sup> and for the even larger oxygen concentration  $c_O = 7$  at. %, it drops down to 52 (m $\Omega$  cm)<sup>-1</sup>. Thus, it appears that, by ion-irradiation, oxygen-stabilized defects can be produced which are especially instrumental in enhancing  $T_c$  for  $c_O \leq 4$  at. %. For higher  $c_O$  values, the production of resistivity by these stabilized defects starts to become dominating resulting in reduced  $\delta t/\rho$  values. Eventually, for approximating  $c_O = 40$  at. %, the metal-insulator transition is approached.<sup>14</sup> This situation has been analyzed by Dynes *et al.*<sup>23</sup> and from their data a slope of  $45 \pm 5$  (m $\Omega$  cm)<sup>-1</sup> is deduced by Belitz.<sup>7</sup> This value is close to ours found for  $c_O = 7$  at. % by irradiation. But, if the experimental ini-

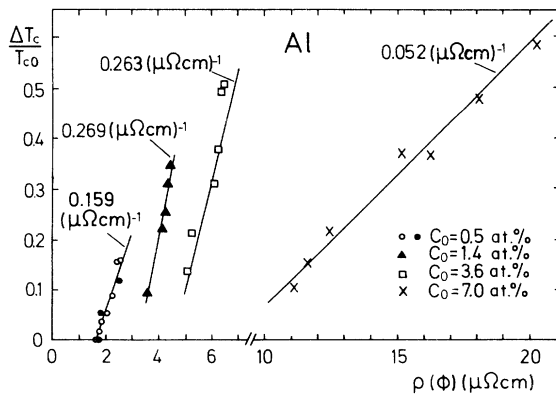


FIG. 4. Relative changes of the superconducting transition temperature  $\Delta T_c/T_{c0}$  induced by low-temperature ( $T < 10$  K) self-ion irradiation ( $Al^{2+}$ , 500 keV) of Al films as a function of the electrical resistivity  $\rho$ . Different symbols stand for different samples. The oxygen content of the films is indicated in the inset.

TABLE II. Input data for  $\alpha$ -Ga and  $\beta$ -Ga.

$\Theta_D$ (K)	$k_F$ ( $10^8$ cm <sup>-1</sup> )	$q_D$ ( $10^8$ cm <sup>-1</sup> )	$\kappa$ ( $10^8$ cm <sup>-1</sup> )	$T_{c0}$ (K)	$\alpha$ -Ga	$\beta$ -Ga	
240 <sup>a</sup>	1.66 <sup>a</sup>	2.1 <sup>a</sup>	1.99 <sup>a</sup>	1.07			
				6.3			
$\ln(E_F/k_B\Theta_D)$	$y = \kappa/2k_F$	$x_D = q_D/2k_F$	$(c_L/c_T)^2$	$\rho_M^{FEM}$ ( $\mu\Omega$ cm)	$(\delta t/\rho)_B$ (1/m $\Omega$ cm)	$(\delta t/\rho)_{KSS}$ (1/m $\Omega$ cm)	$(\delta t/\rho)_{expt}$ (1/m $\Omega$ cm)
6.22 <sup>a</sup>	0.60	0.63	16.3 <sup>b</sup>	733	519	161	545
6.22	0.60	0.37	1.8	733	8	161	(18)
						$\lambda_M = 0.41^c$	$\lambda_0 = 0.26^d$
							255
					$\partial(\delta t/\rho)/\partial y$	$\partial(\delta t/\rho)/\partial x_D$	$\partial(\delta t/\rho)/\partial(c_L/c_T)^2$
					+12.7	-1014	+31.7
							-138

<sup>a</sup>From Ref. 15.

<sup>b</sup>From Ref. 20.

<sup>c</sup>McMillan value.

<sup>d</sup>McMillan value with  $\mu^* = 0$ .

tial slope  $(\delta t/\rho)$  is taken for granular Al films and not the value calculated from the maximum  $T_{c,\max}=2.2$  K and  $\rho(T_{c,\max})=200 \mu\Omega \text{ cm}$ , one obtains  $(\delta t/\rho)=23 (\text{m}\Omega \text{ cm})^{-1}$  from the data of Ref. 23. This is in excellent agreement with our previous result of  $(\delta t/\rho)=24 (\text{m}\Omega \text{ cm})^{-1}$  for granular Al films.<sup>24</sup> But, it should be stressed that all experimental values  $(\delta t/\rho) < 100 (\text{m}\Omega \text{ cm})^{-1}$  appear to be reduced due to the presence of oxygen within the samples. Thus, for a comparison to theory with input parameters corresponding to pure Al, a slope of  $(\delta t/\rho)=159 (\text{m}\Omega \text{ cm})^{-1}$  obtained by irradiation of the purest films seems to be most appropriate. As for the former examples, all input data are collected in Table III. In this table, the theoretical slopes  $(\delta t/\rho)$  as calculated from the theories of Belitz and of Keck and Schmid are also included. The value  $(\delta t/\rho)=180 (\text{m}\Omega \text{ cm})^{-1}$  obtained by using  $\rho_M^{\text{expt}}$  is in good agreement with experiment. This is corroborated by the following error estimates based on the partial derivatives of  $(\delta t/\rho)$  as given in Table III: if a relative error of 5% is assumed for  $x_D$ ,  $y$ , and  $(c_L/c_T)^2$ , one obtains an absolute error  $\Delta(dt/\rho)=\pm 24 (\text{m}\Omega \text{ cm})^{-1}$ , i.e., the experimental value lies within the theoretical range  $(\delta t/\rho)_B=180\pm 24 (\text{m}\Omega \text{ cm})^{-1}$ . The high sensitivity of  $\delta t/\rho$  on  $x_D$  changes as given in Table III suggests, as a natural explanation of the low  $(\delta t/\rho)$  values experimentally observed for oxide-containing granular Al films, the assumption of a reduced electron density resulting in smaller  $k_F$  values.

The data summarized in Table III further indicate a significantly worse agreement of the experimental slope with the calculation according to the theory of Keck and Schmid even when the smaller  $\lambda_0$  values are used. The full calculation [using formula (2.13) of Ref. 7] including  $\mu^*$  is necessary to obtain  $(\delta t/\rho)_B=180 (\text{m}\Omega \text{ cm})^{-1}$ .

A further detail appears to be noteworthy. In Ref. 7, a value of  $(\delta t/\rho)=190 (\text{m}\Omega \text{ cm})^{-1}$  is quoted for quenched-condensed Al deduced from Ref. 8. This value, though being close to the theoretical one, is clearly too large for the same reason as in the case of Zn: a bulk value for  $\rho(273 \text{ K})$  is used, which is not appropriate for films exhibiting a resistance ratio  $r=1.5$ . By performing the same type of experiments, we obtained values ranging between 42 and 46  $(\text{m}\Omega \text{ cm})^{-1}$ .<sup>25</sup> Furthermore, by RBS it could be shown that quench-condensed Al films, which are not prepared under UHV conditions, typically contain 10-at. % oxygen. Thus, the low value of  $(\delta t/\rho)$  is consistent with the results on granular films.

#### D. In

Indium, similar to the case of Ga, exhibits a large ratio of the longitudinal to the transverse velocity of sound  $(c_L/c_T)^2=12$ . Theoretically, this should result in a large- $T_c$  enhancement by disorder. To test this prediction, previous results of irradiation experiments of In films<sup>27</sup> are reanalyzed.

The In-films were evaporated within the irradiation cryostat onto glass substrates held at 200 K. After annealing to RT and recooling to liquid-He temperature, the films were irradiated or implanted with Ar<sup>+</sup> ions (275 and 125 keV, respectively, typical film thickness 70 nm).

TABLE III. Input data for Al.

$\Theta_D$ (K)	$k_F$ ( $10^8 \text{ cm}^{-1}$ )	$q_D$ ( $10^8 \text{ cm}^{-1}$ )	$\kappa$ ( $10^8 \text{ cm}^{-1}$ )	$T_{c0}$ (K)	$\rho_M^{\text{FEM}}$ ( $\mu\Omega \text{ cm}$ )	$A^{\text{expt}}$ ( $10^{-12} \Omega \text{ cm}^2$ )	$\rho_M^{\text{expt}}$ ( $\mu\Omega \text{ cm}$ )	$(\delta t/\rho)_B$ ( $1/\text{m}\Omega \text{ cm}$ )	$(\delta t/\rho)_{\text{KS}}$ ( $1/\text{m}\Omega \text{ cm}$ )	$(\delta t/\rho)_{\text{expt}}$ ( $1/\text{m}\Omega \text{ cm}$ )
428 <sup>a</sup>	1.75 <sup>b</sup>	1.32 <sup>b</sup>	2.05 <sup>b</sup>	1.20						
									$\lambda_M=0.38^f$	$\lambda_0=0.233^g$
5.76 <sup>b</sup>	0.59	0.38	4.13 <sup>c</sup>	695		222	74	121		159
5.76 <sup>b</sup>	0.59	0.38	4.13 <sup>c</sup>	695		180	60	98		
$\partial(\delta t/\rho)/\partial y^e$ $\partial(\delta t/\rho)/\partial x_D$ $\partial(\delta t/\rho)/\partial(c_L/c_T)^2$ $\partial(\delta t/\rho)/\partial T_{c0}$ (K <sup>-1</sup> )										
+1.4   -847   +61   -155										

<sup>a</sup>From Ref. 26.

<sup>b</sup>From Ref. 15.

<sup>c</sup>From Ref. 20.

<sup>d</sup>From Ref. 21.

<sup>e</sup> $\rho = \rho/\rho_M$ .

<sup>f</sup>McMillan value.

<sup>g</sup>McMillan value with  $\mu^*=0$ .

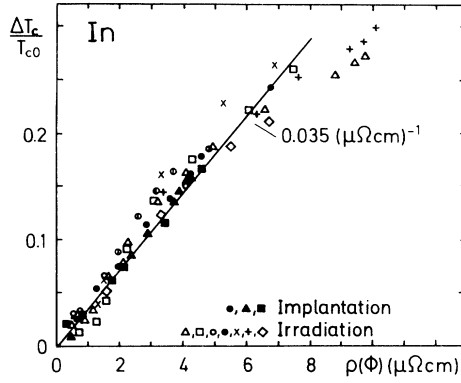


FIG. 5. Relative changes of the superconducting transition temperature  $\Delta T_c/T_{c0}$  induced by low-temperature ( $T < 10$  K)  $\text{Ar}^+$  bombardment of In films as a function of the electrical resistivity  $\rho$ . Different symbols stand for different samples [open symbols, irradiation (275 keV); solid symbols, implantation (125 keV)].

The annealed In films showed large resistance ratios  $r$  with  $10 \leq r \leq 18$  and typical residual resistivities of  $\rho(4.2 \text{ K}) = 0.6 \mu\Omega \text{ cm}$ . The  $T_{c0}$  values of these films were found to be very reproducible with  $T_{c0} = 3.45 \pm 0.03 \text{ K}$  averaged over ten samples. No oxygen impurities could be detected by RBS within the resolution limit. The effect of the  $\text{Ar}^+$  bombardment at  $T < 10 \text{ K}$  on  $T_c$  is presented in Fig. 5, where the relative  $T_c$  change  $\delta t$  is plotted versus the resistivity  $\rho$  for ten different samples (each represented by a different symbol in Fig. 5). Open symbols and crosses stand for irradiation experiments ( $R_p > D$ ) and solid symbols for implantation ( $R_p < D$ ). No specific effect can be distinguished within the scatter of the data due to implanted Ar atoms. The solid line, representing the initial linear  $\delta t$ - $\rho$  behavior, has a slope of  $(\delta t/\rho) = 35 \text{ (m}\Omega \text{ cm)}^{-1}$ . It should be noted that the experimental data for  $\rho \geq 6 \mu\Omega \text{ cm}$  show a significant deviation from the solid straight line indicating that the first-order expansion of McMillan's  $T_c$  formula used in Ref. 7 is no longer appropriate in this case. Earlier results by Heim *et al.*<sup>28</sup> obtained by low-temperature self-ion implantation of In films are in excellent agreement with the data shown in Fig. 5 and confirm the deviation from the straight line for higher resistivities. The results given in Fig. 5 can be compared with those of Bergmann<sup>29</sup> for quench-condensed In films, which were stepwise annealed to reduce the amount of disorder. From these data a slope of  $(\delta t/\rho) = 60 \text{ (m}\Omega \text{ cm)}^{-1}$  has been deduced by Belitz.<sup>7</sup> Clearly, the behavior of quench-condensed In films is different from the results of ion-induced disorder for  $1 \leq \rho \leq 5 \mu\Omega \text{ cm}$ . This is a further example that different preparation techniques can lead to different types of defects, each acting specifically on  $T_c$ .

To compare the experimental results to theory, the input parameters collected in Table IV were used. This table also contains the theoretical results. As can be seen, the free-electron model leads to far too large  $(\delta t/\rho)$  values as compared to experiment. But even if the most probable Mott resistivity  $\rho_M^{\text{expt}} = 1.8 \text{ m}\Omega \text{ cm}$  is used, the

TABLE IV. Input data for In.

$\Theta_D$ (K)	$k_F$ ( $10^8 \text{ cm}^{-1}$ )	$q_D$ ( $10^8 \text{ cm}^{-1}$ )	$\kappa$ ( $10^8 \text{ cm}^{-1}$ )	$T_{c0}$ (K)
112 <sup>a</sup>	1.51 <sup>b</sup>	1.13 <sup>b</sup>	1.90 <sup>b</sup>	3.40
6.79	0.63	0.37	12.0 <sup>c</sup>	806
6.79	0.63	0.37	12.0 <sup>c</sup>	
6.79	0.63	0.37	12.0 <sup>c</sup>	
6.79	0.63	0.37	6.8 <sup>d</sup>	
$\ln(E_F/k_B\Theta_D)$ $y = \kappa/2k_F$ $x_D = q_D/2k_F$ $(c_L/c_T)^2$ $\rho_M^{\text{FEM}}$ ( $\mu\Omega \text{ cm}$ ) $A^{\text{expt}}$ ( $10^{-12} \Omega \text{ cm}^2$ ) $\rho_M^{\text{expt}}$ ( $\mu\Omega \text{ cm}$ ) $(\delta t/\rho)_B$ ( $1/\text{m}\Omega \text{ cm}$ ) $(\delta t/\rho)_{\text{KS}}$ ( $1/\text{m}\Omega \text{ cm}$ ) $(\delta t/\rho)_{\text{expt}}$ ( $1/\text{m}\Omega \text{ cm}$ )				
				$\lambda_M = 0.7^h$ $\lambda = 0.805^f$ $\lambda_0 = 0.50^g$
				279 124 98 67 45 37
				220 151
				1812 2718 1812 54 41
				$\partial(\delta t/\rho)/\partial y^i$ $\partial(\delta t/\rho)/\partial x_D$ $\partial(\delta t/\rho)/\partial(c_L/c_T)^2$ $\partial(\delta t/\rho)/\partial T_{c0}$ ( $\text{K}^{-1}$ )
				+0.67 -936 +24.2 -46.3

<sup>a</sup>From Ref. 26.

<sup>b</sup>From Ref. 15.

<sup>c</sup>From Ref. 20.

<sup>d</sup>Averaged value from Ref. 21.

<sup>e</sup>Averaged value for films from Ref. 21.

<sup>f</sup>From Ref. 33.

<sup>g</sup>From McMillan's formula with  $\mu^* = 0$ .

<sup>h</sup>From McMillan's formula.

<sup>i</sup> $\rho = \rho/\rho_M$

<sup>j</sup>From Ref. 18, calculated from elastic constants.



resulting  $(\delta t/\rho)_B = 124 \text{ (m}\Omega \text{ cm)}^{-1}$  is larger than the experimental value by a factor of 3.5. This discrepancy can be somewhat mitigated by increasing  $\rho_M^{\text{expt}}$  as well as  $\lambda$  up to the highest values reported in the literature for In. But even then, the theoretical value  $65 \text{ (m}\Omega \text{ cm)}^{-1}$  is too large by a factor of 1.9. This disagreement is cured immediately if a lower  $(c_L/c_T)^2$  ratio is accepted. In Ref. 18, a value of 6.8 is given for this ratio, deduced from the elastic constants of In and assuming cubic symmetry. Using this lower value, the resulting theoretical slopes  $(\delta t/\rho)$  are in good agreement with the experimental value (cf. Table IV). By standard error analysis based on the partial derivatives given in Table IV, one derives a total error  $\Delta(\delta t/\rho)_B = 17 \text{ (m}\Omega \text{ cm)}^{-1}$  assuming a 10% error of  $(c_L/c_T)^2$  and a 5% error of  $x_D$ . Thus, an evaluation of the agreement between theory and experiment in the case of In hinges on the accepted value of  $(c_L/c_T)^2$ .

E. Pb

Pb films, disordered by quench condensation at 4.2 K, virtually show no  $T_c$  changes<sup>8</sup> in agreement with cold-worked samples.<sup>30</sup> On the other hand, ion-irradiated Pb foils<sup>31</sup> and thick (4  $\mu\text{m}$ ) films<sup>32</sup> exhibit a small  $T_c$  decrease. Obviously, the disorder-induced  $T_c$  behavior of Pb is very close to the change of sign of  $(\delta t/\rho)$ , which is describable by the theory of Belitz.

Pb films (100 nm) were evaporated from a Ta boat within the irradiation cryostat onto glass substrates held at 125 K (background pressure  $3 \times 10^{-7}$  mbar, deposition rate 7 nm/s). After annealing at 350 K, the films showed high-resistance ratios ( $r = 23$ ) with corresponding residual resistivities of typical  $\rho(4.2 \text{ K}) = 1 \mu\Omega \text{ cm}$ . The average  $T_{c0}$  value was  $7.19 \pm 0.003 \text{ K}$ . These films were irradiated at  $T < 10 \text{ K}$  with 225-keV  $\text{Ar}^+$  ions and the  $T_c$  and  $\rho$  changes were determined *in situ*. The results are shown in Fig. 6, where the relative  $T_c$  changes  $\Delta T_c/T_{c0}$  are plotted versus the resistivity  $\rho$  as obtained by Ar bombardment. A linear  $\delta t/\rho$  behavior is found with a negative slope of  $-5.3 \text{ (m}\Omega \text{ cm)}^{-1}$ . This negative sign

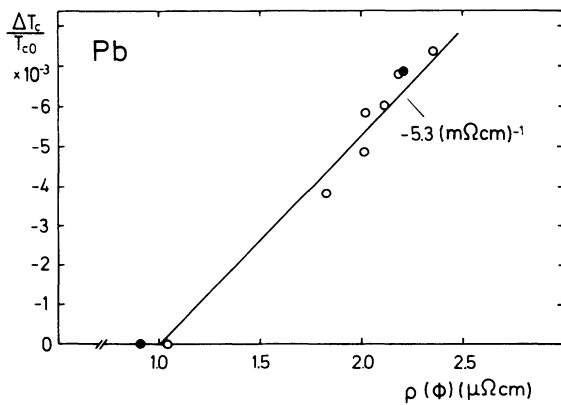


FIG. 6. Relative changes of the superconducting transition temperature  $\Delta T_c/T_{c0}$  induced by low-temperature ( $T < 10 \text{ K}$ )  $\text{Ar}^+$  irradiation (225 keV) of Pb films as a function of the electrical resistivity  $\rho$ . The different symbols stand for different samples.

TABLE V. Input data for Pb.

$\Theta_D$ (K)	$k_F$ ( $10^8 \text{ cm}^{-1}$ )	$q_D$ ( $10^8 \text{ cm}^{-1}$ )	$\kappa$ ( $10^8 \text{ cm}^{-1}$ )	$T_{c0}$ (K)					
105 <sup>a</sup>	1.58 <sup>b</sup>	1.19 <sup>b</sup>	1.95 <sup>b</sup>	7.19					
$\ln(E_F/k_B\Theta_D)$	$y = \kappa/2k_F$	$x_D = q_D/2k_F$	$(c_L/c_T)^2$	$\rho_M^{\text{FM}}$ ( $\mu\Omega \text{ cm}$ )	$A^{\text{expt}}$ ( $10^{-12} \Omega \text{ cm}^2$ )	$\rho_M^{\text{expt}}$ ( $\mu\Omega \text{ cm}$ )	$(\delta t/\rho)_B$ ( $1/\text{m}\Omega \text{ cm}$ )	$(\delta t/\rho)_{\text{KS}}$ ( $1/\text{m}\Omega \text{ cm}$ )	$(\delta t/\rho)_{\text{expt}}$ ( $1/\text{m}\Omega \text{ cm}$ )
6.95	0.62	0.38	8.3 <sup>c</sup>	770	11.9 <sup>d</sup>	1882	$\lambda_M = 1.1^e$	$\lambda = 1.55$	$\lambda = 0.82^f$
6.95	0.62	0.38	8.3			1882	66	27	64
$\mu^* = 0.105$		0.38	5.2 <sup>i</sup>			1882	9.9	-4.4	26
					$\partial(\delta t/\rho)/\partial x_D$	$\partial(\delta t/\rho)/\partial(c_L/c_T)^2$			
					-435	+13.3			

<sup>a</sup>From Ref. 26.  
<sup>b</sup>From Ref. 15.  
<sup>c</sup>From Ref. 20.  
<sup>d</sup>From Ref. 21.  
<sup>e</sup>From McMillan's formula.  
<sup>f</sup>From Ref. 33.  
<sup>g</sup>From McMillan's formula with  $\mu^* = 0$ .  
<sup>h</sup>From Ref. 33.  
<sup>i</sup>From Ref. 34.

TABLE VI. Properties of  $\text{Al}_2\text{Au}$  and  $\text{AuIn}_2$ 

	$\rho$ (77 K) ( $\mu\Omega\text{cm}$ ) <sup>a</sup>	$\rho$ (300 K) ( $\mu\Omega\text{cm}$ )	$T_K$ (K)	$R$ (300 K)/ $R$ (4.2 K)	$(\delta t/\rho)_{\text{expt}}$ ( $\text{m}\Omega\text{cm})^{-1}$	$T_{c0}$ (mK)
$\text{Al}_2\text{Au}$	220±53	48±5 <sup>c</sup>	218±10 <sup>b</sup>	1.2	92.4	180 <sup>d</sup>
$\text{AuIn}_2$	95 <sup>f</sup>	29±5	166±18	1.5	115	210±10 <sup>e</sup>

<sup>a</sup>Value of the amorphous phase.

<sup>b</sup>Crystallization temperature.

<sup>c</sup>Value of the crystalline phase.

<sup>d</sup>From Ref. 35.

<sup>e</sup>From Refs. 35–37.

<sup>f</sup>From Ref. 13.

confirms the earlier results obtained by ion irradiation, which were quoted above. For the comparison of the experimental results to theory, the input parameters collected in Table V were used. In this table, the theoretical results are also given. As generally found, the FEM value of the Mott resistivity results in much too high values of the theoretical slopes  $(\delta t/\rho)$ . But even if the experimental value  $\rho_M^{\text{expt}}$  is used, the resulting  $(\delta t/\rho)=27$  ( $\text{m}\Omega\text{cm})^{-1}$  based on McMillan's formula is significantly too large. Part of this discrepancy can be reduced by assuming the experimental value  $\lambda=1.55$  for Pb leading to  $(\delta t/\rho)=9.9$  ( $\text{m}\Omega\text{cm})^{-1}$ . Though this result approximately lies within the calculated errors [a total error  $\Delta(\delta t/\rho)=\pm 11$  ( $\text{m}\Omega\text{cm})^{-1}$  is deduced by standard error analysis based on the dominating partial derivatives given in Table V and assuming a 10% error of  $x_D$  and  $(c_L/c_T)^2$ ], it exhibits a similar trend as observed for In: high experimental values of  $(c_L/c_T)^2$  lead to an overestimate of  $(\delta t/\rho)$  by theory. If  $(c_L/c_T)^2=5.2$  is chosen, a value given in Ref. 34 as calculated from elastic constants, and the experimental values of  $\mu^*$  and  $\lambda$  are used, one obtains  $(\delta t/\rho)_B=-4.4$  ( $\text{m}\Omega\text{cm})^{-1}$  in good agreement with the experimental result.

#### F. $\text{Al}_2\text{Au}$ and $\text{AuIn}_2$

In the following, the effect of irradiation-induced disorder on  $T_c$  of the isostructural ( $\text{CaF}_2$  structure) intermetallic compounds  $\text{Al}_2\text{Au}$  and  $\text{AuIn}_2$  are reported. Both are weak-coupling superconductors with transition temperatures of 180 mK (Ref. 35) and  $210\pm 10$  mK,<sup>35–37</sup> respectively. Furthermore, like  $\alpha$ -Ga, both systems can be forced into an amorphous phase by low-temperature ion bombardment<sup>38,39</sup> in a continuous way.

As described in Sec. II, the alloy films were flash evaporated within the irradiation cryostat onto substrates held at 77 K (typical film thicknesses were 60 and 40 nm, respectively). This procedure results in an amorphous phase for both systems. Next, the films were recrystallized [ $T_K=220\pm 53$  K for  $a$ - $\text{Al}_2\text{Au}$  and  $T_K=(166\pm 18)$  K

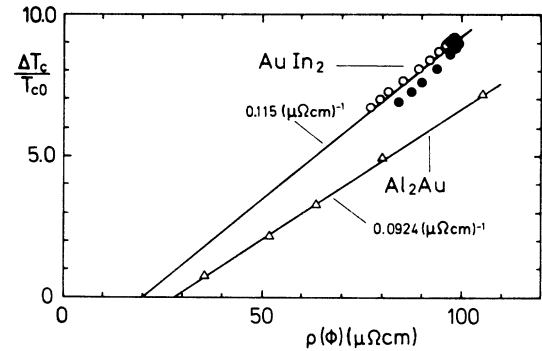


FIG. 7. Relative changes of the superconducting transition temperature  $\Delta T_c/T_{c0}$  induced by low-temperature ( $T < 10$  K)  $\text{Ar}^+$  (300 keV, open circles) and  $\text{He}^+$  irradiation (350 keV, solid circles) of  $\text{AuIn}_2$  and  $\text{Ar}^+$  irradiation (250 keV) of  $\text{Al}_2\text{Au}$  films as a function of the electrical resistivity  $\rho$ . The different symbols stand for different samples.

for  $a$ - $\text{AuIn}_2$ ] and annealed at 300 K. After recooling, the samples were irradiated at  $T < 10$  K with  $\text{Ar}^+$  ions (250 keV for  $\text{Al}_2\text{Au}$ , 300 keV for  $\text{AuIn}_2$ ) and  $\text{He}^+$  ions (350 keV for  $\text{AuIn}_2$ ). The resistivity  $\rho$  and  $T_c$  were determined *in situ*. The results of these experiments are presented in Fig. 7, where  $\Delta T_c/T_{c0}$  is plotted versus the resistivity  $\rho$  for both systems. As in Ga, a linear  $\delta t$ -vs- $\rho$  behavior is observed over the full range from the polycrystalline to the amorphous phase. This indicates that, to a first approximation, the disorder, which influences  $T_c$ , can be characterized by the corresponding resistivity independent of specific types of the defects present. Since the input data necessary for a comparison to theory are not available for both compounds, in Table VI only their characteristic properties as determined experimentally are collected. The experimental slopes  $(\delta t/\rho)$  will be compared to theory in the following section.

TABLE VII. Input parameters for the  $(\delta t/\rho)$ -vs- $T_{c0}$  curves in Fig. 8 representing simple metals.

$\Theta_D$ (K)	$\ln(E_F/k_B\Theta_D)$	$y$	$x_D$	$(c_L/c_T)^2$	$\rho_M$ ( $\mu\Omega\text{cm}$ )	
200	5.0	0.5	0.30	1.8	750	Solid line in Fig. 8
250	5.0	0.5	0.34	3.0	800	Dashed line in Fig. 8

### G. Representative $(\delta t/\rho)$ -vs- $T_{c0}$ curves

In cases where no experimental input parameters are available to allow a calculation of  $(\delta t/\rho)$ , one is restricted to representative  $(\delta t/\rho)$ -vs- $T_{c0}$  curves giving at least the expected trends for a specific class of superconductors. Belitz has introduced two curves, one representing transition metals and their alloys, the other representing simple metals and their alloys. In our case, the latter is more appropriate. This curve is shown in Fig. 8 by the solid line together with a second curve (dashed) calculated with a different set of input parameters. These parameters are given in Table VII. Also added to Fig. 8 are the results of all superconductors studied in the present work. Except for  $\alpha$ -Ga and the alloys AuIn<sub>2</sub>, Al<sub>2</sub>Au, experimental input parameters were available resulting in a satisfying agreement with theory as has been shown in the previous sections. This agreement is reflected in Fig. 8. With only one exception ( $\alpha$ -Ga), all experimental data including the alloys and  $\beta$ -Ga are close to the two representative curves confirming the overall trend as calculated by the Belitz theory. More specifically, the input parameters given in Table VII allow a quantitative estimate of  $(\delta t/\rho)$  with a reasonable accuracy for systems which can be modeled as simple metals. The extremely large value of  $(\delta t/\rho)$  experimentally found for  $\alpha$ -Ga is a consequence of the

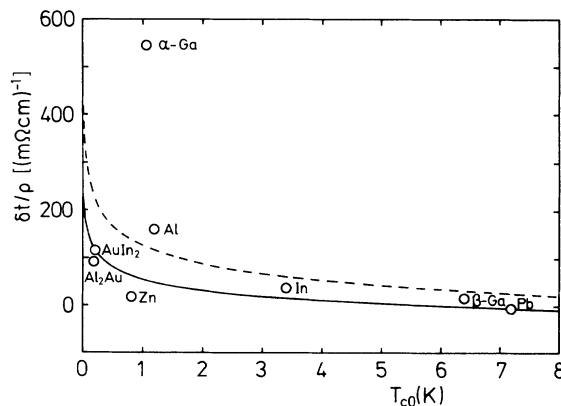


FIG. 8. Slopes of the linear  $\delta t = \Delta T_c / T_{c0}$ -vs- $\rho$  relations as a function of the transition temperature  $T_{c0}$  of the disorder-free material. The solid and dashed curves are theoretical results after Belitz (Ref. 7) calculated with the input parameters given in Table VII. The open circles are the experimental results of the present study.

anomalously high anisotropy of the sound velocities as discussed in Sec. II. Due to this anomaly,  $\alpha$ -Ga cannot be taken as a typical simple metal with a superconducting behavior as represented by the curves in Fig. 8.

### IV. CONCLUSIONS

We have analyzed the influence of disorder on the superconducting transition temperature  $T_c$  for eight systems representing simple metals or alloys. For this purpose, the samples were irradiated at low temperature and the corresponding changes  $\Delta T_c$  were observed *in situ*. In all cases, a resistivity range is found with a linear  $\Delta T_c$ -vs- $\rho$  behavior as expected by theory. The corresponding slopes  $(\delta t/\rho)$  are compared to the theory of Belitz and good agreement is obtained if input parameters are used, which are specific for each system. But, due to the uncertainty of these parameters, this agreement does not exclude  $T_c$ -influencing mechanisms like changes of the phonon spectra, which are not taken into account by the above theory. Nevertheless, the general trend of  $(\delta t/\rho)$ -vs- $T_{c0}$  found by Belitz is nicely confirmed by the present results.

In some cases, by repeating quench-condensation experiments under improved vacuum conditions, discrepancies concerning the numerical value of  $(\delta t/\rho)$  could be resolved. Especially, the influence of oxygen impurities on this value has been clearly demonstrated. A further remarkable result is obtained for systems which can be forced into the amorphous state by ion irradiation. Even in this case, a continuous  $\delta t$ -vs- $\rho$  behavior is observed confirming the notion of a universal influence of disorder on  $T_c$ . But, it turns out that this description is only an approximation, though a very good one. Clear evidence could be provided that different defects produced by different preparation techniques influence  $T_c$  differently, leading to a deviation from universality.

### ACKNOWLEDGMENTS

We would like to thank T. Habisreuther and A. Plewnia for experimental assistance. This work was supported by Deutsche Forschungsgemeinschaft (DFG) within SFB 306.

<sup>1</sup>P. W. Anderson, J. Phys. Chem. Solids **11**, 26 (1959).

<sup>2</sup>B. Keck and A. Schmid, J. Low Temp. Phys. **24**, 611 (1976).

<sup>3</sup>L. R. Testardi and L. F. Mattheiss, Phys. Rev. Lett. **41**, 1612 (1978).

<sup>4</sup>P. W. Anderson, K. A. Muttalib, and T. V. Ramakrishnan, Phys. Rev. B **28**, 117 (1983).

<sup>5</sup>D. A. Browne, K. Levin, and K. A. Muttalib, Phys. Rev. Lett. **58**, 156 (1987).

<sup>6</sup>(a) D. Belitz, Phys. Rev. B **35**, 1636 (1987); (b) D. Belitz, *ibid.* **35**, 1651 (1987).

<sup>7</sup>D. Belitz, Phys. Rev. B **36**, 47 (1987).

<sup>8</sup>W. Buckel and R. Hilsch, Z. Phys. **138**, 109 (1954).

<sup>9</sup>G. Bergmann, Phys. Rep. C **27**, 159 (1976).

<sup>10</sup>J. F. Ziegler, J. P. Biersack, and U. Littmark, *The Stopping and Range of Ions in Matter* (Pergamon, New York, 1985).

<sup>11</sup>W. Bauriedl, G. Heim, M. Hitzfeld, P. Ziemann, and W. Buckel, Nucl. Instrum. Methods **189**, 145 (1981).

<sup>12</sup>W. Folberth, H. Leitz, and J. Hasse, Z. Phys. B **43**, 235 (1981).

<sup>13</sup>E. Compans, P. Häussler, and F. Baumann, Verh. Dtsch. Phys. Ges. **16**, 490 (1981); P. Häussler, Z. Phys. B **53**, 15 (1983).

<sup>14</sup>P. Ziemann, O. Meyer, G. Heim, and W. Buckel, Z. Phys. B **35**, 141 (1979).

<sup>15</sup>N. W. Ashcroft and N. D. Mermin, *Solid State Physics* (Saunders College, Philadelphia, 1976).

<sup>16</sup>J. M. Ziman, *Electrons and Phonons* (Oxford University, Ox-

- ford, 1972).
- <sup>17</sup>U. Görlach, P. Ziemann, and W. Buckel, Nucl. Instrum. Methods **209/210**, 235 (1983).
- <sup>18</sup>R. Tidecks, *Nonequilibrium Phenomena in Superconductors*, Springer Tracts in Modern Physics, Vol. 121 (Springer-Verlag, Berlin, 1990).
- <sup>19</sup>M. Holz, P. Ziemann, and W. Buckel, Phys. Rev. Lett. **51**, 1584 (1983).
- <sup>20</sup>W. Schaaffs, Landolt-Börnstein, New Series, Group II, Vol. 5, Pt. 5 (Springer-Verlag, Berlin, 1967), p. 234.
- <sup>21</sup>J. Bass, Landolt-Börnstein, New Series, Group III, Vol. 15b, Part 1.3 (Springer-Verlag, Berlin, 1985), p. 139.
- <sup>22</sup>G. Deutscher, H. Fenichel, M. Gershenson, E. Grünbaum, and Z. Ovadyahu, J. Low Temp. Phys. **10**, 231 (1973).
- <sup>23</sup>R. C. Dynes and J. P. Garno, Phys. Rev. Lett. **46**, 137 (1981).
- <sup>24</sup>P. Ziemann, G. Heim, and W. Buckel, Solid State Commun. **27**, 1131 (1978).
- <sup>25</sup>M. Nittmann, P. Ziemann, and W. Buckel, Z. Phys. B **41**, 211 (1981).
- <sup>26</sup>W. L. McMillan, Phys. Rev. **167**, 166 (1968).
- <sup>27</sup>A. Hofmann, P. Ziemann, and W. Buckel, Nucl. Instrum. Methods **182/183**, 943 (1981).
- <sup>28</sup>G. Heim, W. Bauriedl, and W. Buckel, J. Nucl. Mater. **72**, 263 (1978).
- <sup>29</sup>G. Bergmann, Z. Phys. **228**, 25 (1969).
- <sup>30</sup>G. V. Minnigerode, Z. Phys. **154**, 442 (1959).
- <sup>31</sup>F. Ochmann and B. Stritzker, Nucl. Instrum. Methods **209/210**, 831 (1983).
- <sup>32</sup>S. Klaumünzer, G. Ischenko, H. Adrian, and H. Neumüller, J. Low Temp. Phys. **36**, 89 (1979).
- <sup>33</sup>P. B. Allen and R. C. Dynes, Phys. Rev. B **12**, 905 (1975).
- <sup>34</sup>P. B. Allen and M. L. Cohen, Phys. Rev. **187**, B525 (1969).
- <sup>35</sup>D. van Vechten, L. B. Holdemann, R. J. Soulen, Jr., and J. Toots, J. Low Temp. Phys. **51**, 329 (1983).
- <sup>36</sup>K. Gloos, R. König, P. Smeibidl, and F. Pobell (private communication).
- <sup>37</sup>E. Bucher, E. Ehrenfreund, A. C. Gossard, K. Andres, J. H. Wernick, J. P. Maita, A. S. Cooper, and L. D. Longinotti, in *Proceedings of the 13th International Conference on Low Temperature Physics, 1972* (Plenum, New York, 1974), p. 648.
- <sup>38</sup>A. Schmid and P. Ziemann, Nucl. Instrum. Methods B **7/8**, 581 (1985).
- <sup>39</sup>W. Miehle, A. Plewnia, and P. Ziemann, Nucl. Instrum. Methods B **59/60**, 410 (1991).